Journal of Aerosol Science 95 (2016) 43–53

Contents lists available at ScienceDirect

Journal of Aerosol Science

journal homepage: www.elsevier.com/locate/jaerosci

A prototype personal aerosol sampler based on electrostatic precipitation and electrowetting-on-dielectric actuation of droplets

T.G. Foat [a,*], W.J. Sellors [a], M.D. Walker [a], P.A. Rachwal [a], J.W. Jones [a], D.D. Despeyroux [a], L. Coudron [b], I. Munro [b], D.K. McCluskey [b], C.K.L. Tan [b], M.C. Tracey [b]

[a] Dstl, Porton Down, Salisbury, Wiltshire SP4 0JQ, United Kingdom
[b] School of Engineering and Technology, University of Hertfordshire, College Lane, Hatfield, Hertfordshire AL10 9AB, United Kingdom

ARTICLE INFO

Article history:
Received 4 August 2015
Received in revised form
2 December 2015
Accepted 13 January 2016
Available online 23 January 2016

Keywords:
Aerosol collection
Electrostatic precipitator
Electrowetting-on-dielectric
EWOD
Personal sampler

ABSTRACT

An electrostatic precipitator (ESP) based personal sampler with a laboratory based electrowetting-on-dielectric (EWOD) concentrator could provide a high concentration rate personal aerosol sampler system. A prototype system has been developed based on the concept of a lightweight personal ESP collecting aerosol particles onto a hydrophobic surface followed by the use of an EWOD actuated droplet system to transfer the deposited sample into a microlitre size water droplet.

A personal sampler system could provide military or civilian personnel with a wide area biological monitoring capability supplying information on who has been infected, what they have been infected with, how much material they were exposed to and possibly where and when they were infected. Current commercial-off-the-shelf (COTS) personal sampler solutions can be bulky and use volumes of water to extract the sample that are typically a thousand times greater than the proposed method.

Testing of the prototype ESP at a sample flow rate of 5 L min^{-1} demonstrated collection efficiencies greater than 80% for sodium fluorescein particles larger than 4 μm diameter and of approximately 50% at 1.5 μm. The ESP-EWOD system collection efficiency measured for *Bacillus atrophaeus* (BG) spores with an air sample flow rate of 20 L min^{-1} was 2.7% with a concentration rate of 1.9×10^5 min^{-1}. This was lower than expected due to the corona ions from the ESP affecting the hydrophobicity of the collection surface and hence the EWOD efficiency. However, even with this low efficiency the concentration rate is more than an order of magnitude higher than the theoretical maximum of the best current COTS personal sampler. For an optimised system, ESP-EWOD system efficiency should be higher than 32% with a comparable increase in concentration rate.

1. Introduction

Personal samplers have been used for many years in fields such as occupational hygiene to measure individual exposures to toxic materials. A description of a range of personal samplers is given by Vincent (2007) and results from laboratory

* Corresponding author.
E-mail address: tgfoat@dstl.gov.uk (T.G. Foat).

http://dx.doi.org/10.1016/j.jaerosci.2016.01.007
0021-8502/

testing of a range of samplers are presented in Gorner, Simon, Wrobel, Kauffer, and Witschger (2010) and Sleeth and Vincent (2012). However, personal samplers are still not widely used by the military to collect samples to confirm a soldier's exposure to potentially dangerous aerosol such as biological warfare agents (BWAs). Using personal samplers to inform whether soldiers or civilian personnel have been exposed to hazardous levels of BWAs is particularly challenging. This is because the infectious or toxic thresholds of some materials of interest are very low and the equipment used to detect the sampled agents in the field may have relatively high limits of detection.

1.1. High concentration rate personal sampler concept

Biological agents can have very low infectious doses. For example, for *Yersinia pestis*, the causative agent of plague, it is 100 to 500 organisms, and for the smallpox Variola virus, 10 to 100 organisms (Franz, Jahrling, & Friedlander, 1997), meaning that someone can become infected following a very limited exposure. The probability of detection is a function of both the limit of detection or sensitivity of the sensor and the concentration of the target biological agent presented to the sensor. To improve the likelihood of a personal sampler based detection system indicating whether a person has been exposed to a biological agent, it is important that the concentration of the liquid sample is as high as possible. This can be achieved through a high air sample rate or by producing a small output liquid volume. Personal samplers tend not to be suitable for very high flow rate sampling due to physical size constraints and the requirement to run from batteries for long periods; therefore a small liquid output volume is required.

The concentration rate, R_c [min^{-1}] used in the paper is as defined by Han, An, and Mainelis (2010) and is given by

$$R_c = \frac{Q}{V}\eta_s, \tag{1}$$

where Q [$\mathrm{m}^3\ \mathrm{s}^{-1}$] is the air sample flow rate, V [m^3] is the volume of the final liquid sample produced and η_s [dimensionless] is the total system efficiency which includes any efficiencies associated with the collection of the sample or the transfer of the sample into liquid.

The theoretical maximum concentration rate is calculated by assuming all the efficiencies of the sampler are 100%. For a fixed sampling period and mean airborne concentration, a higher value of R_c leads to an increased liquid concentration.

Most COTS personal samplers operate at low air flow rates ($< 5\ \mathrm{L\ min}^{-1}$). For example the Institute of Occupational Medicine (IOM) personal inhalable aerosol sampler (SKC Inc., PA, USA) operates at $2\ \mathrm{L\ min}^{-1}$ and the Button personal inhalable aerosol sampler (SKC Inc., PA, USA) operates at $4\ \mathrm{L\ min}^{-1}$. There are some exceptions such as the recently discontinued BioBadge® (FLIR®, Arlington, VA, USA) which samples at $40\ \mathrm{L\ min}^{-1}$, and the CIP 10-M (developed by Institut National de Recherche et de Sécurité (INERIS)) and the Personal Environmental Monitor (SKC Inc., PA, USA) which both operate at up to $10\ \mathrm{L\ min}^{-1}$.

All COTS personal samplers require or use greater than 1 mL volumes of liquid either to collect the sample into or to wash the collection media. The CIP 10-M uses 2 mL to 2.5 mL (Gorner, Fabries, Duquenne, Witschger, & Wrobel, 2006), BioBadge® uses 5 mL (Ryan, Wright, & Gloster, 2009) and the IOM uses 10 mL (SKC).

The high concentration rate ESP-EWOD concept is based on a lightweight personal ESP to collect aerosol particles onto a removable hydrophobic surface. After the sample has been collected, the hydrophobic surface is placed in an EWOD droplet actuation system. The EWOD system transfers the collected sample into a microlitre size water droplet (2 μL to 3 μL) that is actuated across the surface (Jonsson-Niedziolka et al., 2011), providing a highly concentrated sample for analysis. Table 1 compares the operating parameters of a range of COTS, discontinued or advanced development personal samplers to the ESP-EWOD concept. Two rows are included for the ESP-EWOD concept to show concentration rate when it is operated at $5\ \mathrm{L\ min}^{-1}$ or $20\ \mathrm{L\ min}^{-1}$. It shows that the theoretical maximum concentration rate for the ESP-EWOD concept is several orders of magnitude higher than that of the next highest sampler. It should, however, be noted that the prototype ESP-

Table 1
Operating characteristics for a selection of personal samplers. The concentration rate figures are theoretical maximum values assuming $\eta_s = 100\%$.

Sampler	Air sampling rate/L. min^{-1}	Liquid collection volume /mL	Theoretical maximum concentration rate/min^{-1}	Source of information
BioBadge®	40	5	8.0×10^3	Ryan et al. (2009) and Flir (2014)
CIP-10-M	10	2	5.0×10^3	Gorner et al. (2006) and Arelco (2014)
IOM	2	10	2.0×10^2	SKC
SKC button sampler	4	10	4.0×10^2	Air sample rate (SKC, 2014a). Liquid volume estimated.
Personal environmental monitor	10	10	1.0×10^3	Air sample rate (SKC, 2014b). Liquid volume estimated.
Ilochip	0.12–0.14	0.025	5.2×10^3	Christensen et al. (2009)
ESP-EWOD	5	0.0029	1.7×10^6	This paper
	20	0.0029	6.9×10^6	

EWOD system described in this study only achieved a mean concentration rate of 4.4×10^5 min^{-1} when operated at 20 L min^{-1}.

An important consideration for this personal sampler concept is that the detection system must be able to cope with the small volume liquid samples that are produced. A number of biosensing techniques have been demonstrated using EWOD systems and droplets smaller than 3 μL (Delattre et al., 2012; Kirby & Wheeler, 2013; Nelsen et al., 2010).

An ESP-EWOD based personal sampler system has the additional advantage that, as the transfer of the collected sample into a water droplet is an inherent part of the process, it would lend itself well to automation and integration with a lab-on-a-chip type identification system.

1.2. A review of electrostatic precipitators suitable for use as a personal sampler

There are currently no ESPs described in the open literature that meet the requirements for the ESP component of an ESP-EWOD system. Handheld or small ESPs have been developed by a number of workers previously. These include:

- Nano-aerosol precipitators (Miller, Frey, King, & Sunderman, 2010; Qi, Chen, & Greenberg, 2008).
- A collector employing a superhydrophobic collection channel (Han & Mainelis, 2008; Han et al., 2010) achieving a concentration rate of up to 1.2×10^6 min^{-1} for particles larger than approximately 3 μm.
- A system with a continuously pumped liquid reservoir (Tan, Shen, Yao, & Zhu, 2010).
- Co-axial design ESPs (Quinton, Achard, & Roux, 2013; Volckens, Leith, Boundy, & Hands, 1999, 2000), the latter of which uses the corona wind to induce the sample air flow and has been developed into the Biodosi personal sampler system (Sarda-Esteve, Roux, Sciare, Delapierre, & Nadal, 2012) by the Commissariat à l'énergie atomique et aux énergies alternatives (CEA).

A number of larger, higher flow rate ESPs have been developed for biological aerosol sampling applications where a liquid sample is required (e.g. Clark, Foat, Walker, & Preston, 2008; Roux, Kaspari, Heinrich, Hanschmann, & Grunow, 2013). Methods have also been described for collection of aerosol directly onto cell culture plates using electrostatic precipitation (Mainelis et al., 2002; Sillanpää, Geller, Phuleria, & Sioutas, 2008).

The deficiencies of the ESPs described above in relation to this particular personal sampler application are as follows: they are either physically too large, are designed for nano-aerosol only, have an open liquid reservoir, collect onto a cylindrical surface (which would prevent simple actuation of the EWOD droplet) or have too low an air flow rate. Also, apart from the collector described by Han and Mainelis (2008) and Han et al. (2010) which requires a particular physical orientation, they all have too low a concentration rate. A bespoke ESP is therefore required.

The design and testing of a new personal aerosol sampler based on the ESP-EWOD concept is presented here. The design and testing methodology for the ESP and the EWOD components are described in Sections 2 and 3. Testing included characterisation of the ESP collection efficiency (using sodium fluorescein aerosol and *Bacillus atrophaeus* (BG) spores); measurement of the EWOD surface cleaning efficiency; assessment of how the surface density of the aerosol deposit affects the droplet actuation efficiency and finally the performance of the ESP-EWOD system as a whole.

2. Design

2.1. Design of the electrostatic precipitator

The electrostatic precipitator was designed to operate with a flow rate of 5 L min^{-1}, to have high collection efficiency over the inhalable aerosol diameter range, in this case defined as 1 μ*m to* 20 μm, and to reject larger unwanted particles that may have a negative effect on the EWOD droplet actuation. The ESP should be able to run on batteries for approximately eight hours or more (at room temperature). It should be easy to introduce and remove the collection surface for transfer to the EWOD system. The ESP should be designed so that it could also be used without an EWOD droplet actuation system with the collection surface being washed manually to remove the sample.

The operating principle of the ESP is as follows (Fig. 1 shows the ESP components). Air is drawn in from the environment and passes through a size selective inlet which uses a porous foam to trap larger particles and fibres, while presenting only a moderate pressure drop. The air is drawn into the ESP by a micro fan located at the downstream end of the unit. The aerosol particles are charged using multiple corona needles. The field forming electrode, on the same side but downstream of the corona needles, is fixed in place. The counter electrode for the corona needles and the field forming electrode, acts as the ESP collection electrode. The collection electrode consists of a hydrophobic surface which is held in a removable carrier. The ESP is powered by standard AA batteries and uses COTS modules to step-up to the high potential difference required. The field forming and counter electrodes are at the same voltage but of opposite polarity so the centre of the ESP channel is nominally at ground potential. This was done to reduce the likelihood of positive or negative particles being repelled from the ESP.

Three versions of the ESP were produced, all based around the same configuration of the corona pins and precipitation electrodes. The design moved from more modular proof of concept systems (V1 & V2) to a 3D printed wearable unit (V3). V1

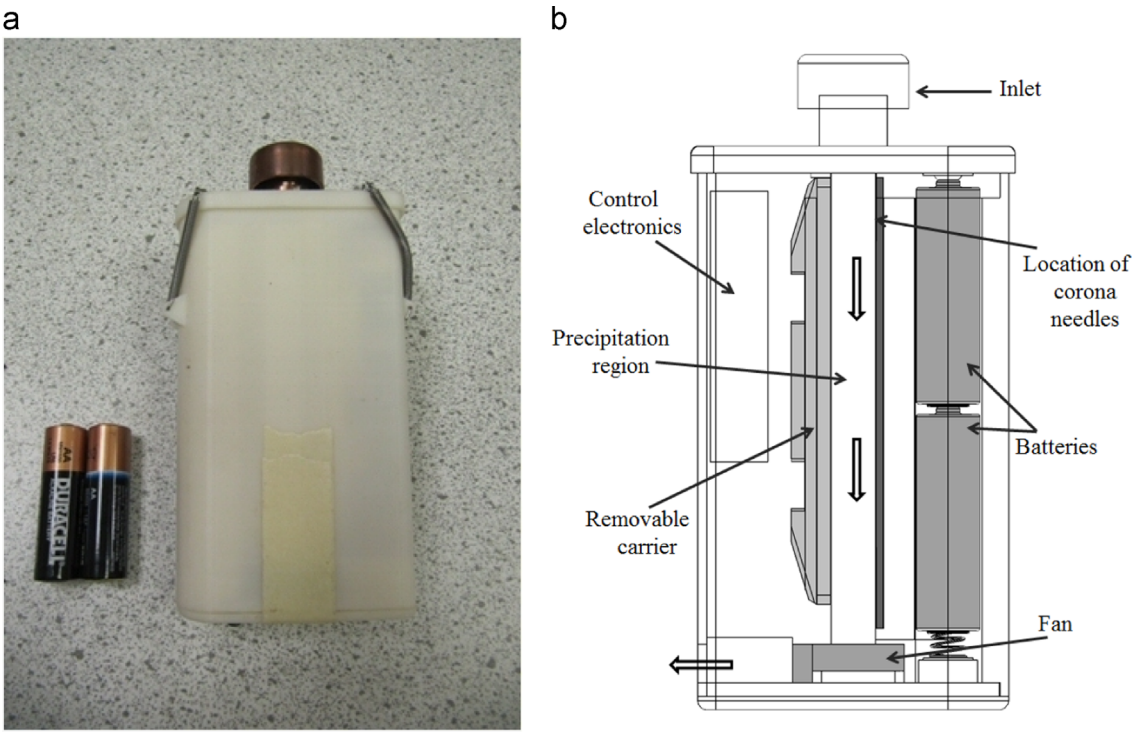

Fig. 1. The ESP V3. (a) is a photograph of the sampler with two AA batteries for scale and (b) is a computer aided design image of the sampler showing the internal components. The hollow arrows indicate the flow path.

was used to determine the corona pin size and number, the ESP geometry and the electrode and material requirements. A photograph and the internal layout of the V3 ESP is shown in Fig. 1. The precipitation electrodes and the corona pins were supplied with ± 4.7 kV by stepping up the battery supply voltage using either a pair of Q101 (-5R & N-5R) modules (EMCO High Voltage Corporation, USA) for V1 & V2 or a pair of smaller, lower current Q60 modules for V3. V1 & V2 were powered from a laboratory power supply and V3 by two AA batteries.

Printed circuit boards (PCBs) were used as the counter electrode and field forming electrode for V1 & V2. The counter electrode was a hydrophobic surface held in a removable carrier for V3.

The air flow was provided by a separate compressed air supply for V1 and a miniature centrifugal blower (STB2008 3.3 V, Strikefan Electronics Co. Ltd., Taiwan) for V2 & V3. The blower was chosen as it was small enough (20.5 mm $\times$ 25.7 mm $\times$ 8.5 mm) and of sufficiently low power, while being able to cope with the moderate pressure drop presented by a porous foam inlet.

The aerosol inlet was a straight metal tube for V1 with a porous foam inlet included for V2 and V3. The selection of the foam was based on methods reported in Vincent, Aitken, and Mark (1993) and Kenny, Aitken, Beaumont, and Gorner (2001). A simple rain cap to prevent rain or other objects dropping into the collector was also included.

A theoretical model, based on Cross (1987) and Rose and Wood (1956) as shown in (2) was used in the design phase to predict the performance of the ESP:

$$\eta_c = \left[1 - \exp\left(-\frac{l/U}{h/U_p}\right)\right]\eta_{c,max} \tag{2}$$

where η_c [dimensionless] is the collection efficiency, defined as the ratio of mass of aerosol collected by the ESP to that collected on a reference filter, l [m] is the length of the collection electrode, U [m s^{-1}] is the mean air velocity through the ESP, h [m] is the separation between the field forming and counter electrodes, and U_p [m s^{-1}] is the drift velocity of the particle in the electric field. U_p was calculated according to Cross (1987). The equation was modified from that given by Rose and Wood to include the likely practical maximum collection efficiency, $\eta_{c,max}$, which in this case was set at 0.85, based on previous experience of designing ESPs. It is the authors' view that the sub-optimal collection efficiency is in part due to the unintentional charging of insulating surfaces within the ESP.

2.2. Design of the EWOD system

The ESP-EWOD concept requires an EWOD droplet (in air) actuation system to concentrate aerosol that has been precipitated onto a hydrophobic surface, into a water droplet. EWOD droplet actuation, and specifically the transfer of

deposited aerosol into an actuated droplet, has been demonstrated previously (Fair, Khlystov, Srinivasan, Pamula, & Weaver, 2004; Jonsson-Niedziolka et al., 2011; Zhao & Cho, 2006). Using EWOD droplet actuation to transfer the precipitated sample into a water droplet has advantages over simpler methods, such as washing the collection surface in a larger volume of liquid. For example, the sample will be highly concentrated into a very small (microlitre size) volume of liquid. In addition, the electrowetting AC process creates flows within the droplet (Ko, Lee, & Kang, 2008), as well as oscillations near the contact line (Oh, Ko, & Kang, 2008). These effects may act to improve the efficiency of deposited particle removal from the surface (Jonsson-Niedziolka et al., 2011) compared to a droplet which is manually moved across the surface or rolled under gravity.

The EWOD system used for this work has the following requirements:

- Include a simple method to receive the surface from the ESP.
- Automatically deliver a water droplet to the EWOD surface for actuation.
- Present the droplet post actuation for pipetting.
- Detect the location of the droplet on the electrode array.
- Indicate whether a droplet has been dispensed and is being successfully actuated.
- Include a system to avoid droplet sticking.
- Be robust and reliable.

EWOD droplet actuation systems are a relatively recent technological development and there are few systems available. Kim et al. (2011) have developed a system to act as a fluid distribution hub. Using multiple liquid delivery points and a cannula to remove waste droplets; droplet actuation was monitored using a microscope. Ningsi (2014) and Choi et al. (2013) describe an integrated digital micro-fluidic platform developed for immunoassays, using 80 actuation electrodes with reservoir and waste electrodes and employing the droplet-in-air approach. Advanced Liquid Logic (part of Illumina, Morrisville, NC, USA) produce custom digital micro-fluidic systems based on electrowetting for fluid handling, mixing etc. and market the LSD-100 Lysosomal Storage Enzyme Analyzer for research use. All reported Advance Liquid Logic systems are droplet-in-oil based. None of the integrated systems are targeted at removing previously deposited material from a surface, a bespoke EWOD system was therefore required.

The EWOD system, including a close up of the base electrodes for EWOD, is shown in Figs. 2 and 3. In Figs. 2b and 3a it can be seen how the carrier with the hydrophobic surface from the ESP is loaded into the EWOD system. The water droplet is delivered from the Eppendorf Tube® water reservoir to the electrodes via plastic tubing and finally a cannula, the cut out for which can be seen at the top left of Fig. 3b. The control electronics are contained in the bottom of the unit and the top and the bottom are connected via a ribbon cable. The system was powered and controlled via a USB connection to a laptop. A bespoke software package was produced to operate the system allowing the user to calibrate the system for droplet detection, deliver a droplet and actuate it across the electrodes, change actuation and droplet sticking avoidance parameters and view the location of the droplet.

2.2.1. *Reliability*

Two different failure mechanisms, electrochemical etching of the electrode and breakdown of the dielectric layer, can cause the droplet actuation to stop.

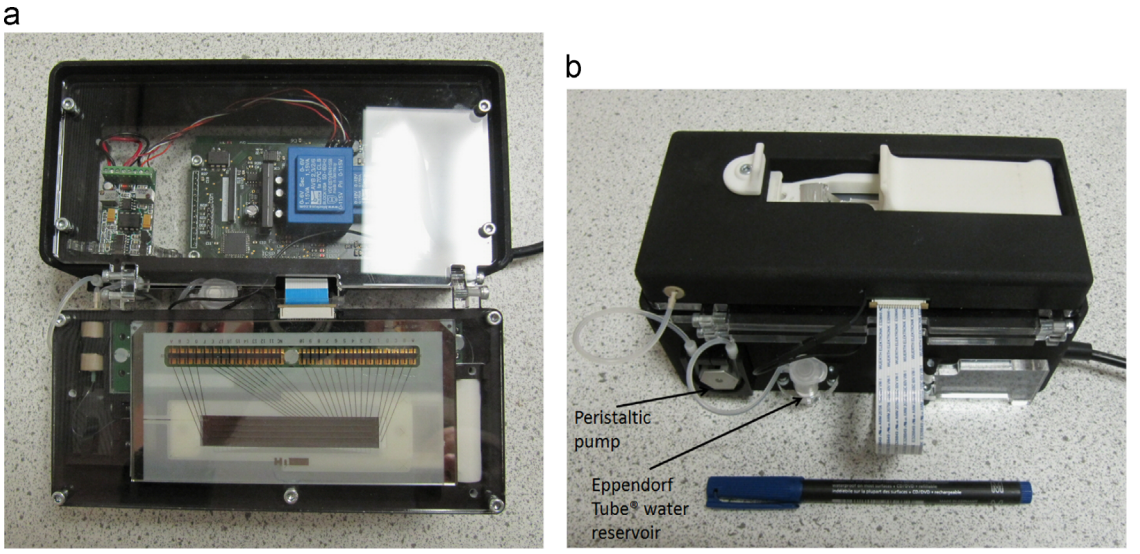

Fig. 2. The EWOD electrode surface and electronics (a) and the top view (b) of the EWOD system.

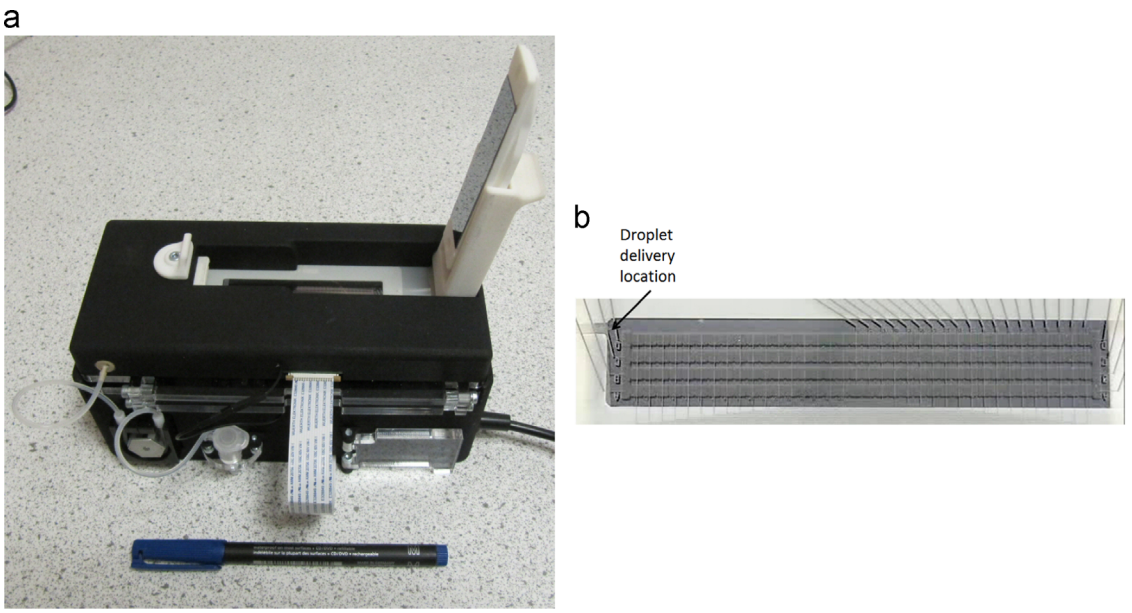

Fig. 3. The top view of the EWOD system with the carrier receiver open showing the exposed hydrophobic surface (a) and the electrode array (b). There are four rows of 19 electrodes with four end electrodes on either side. The cut away for the cannula to deliver the droplet is highlighted. Only 19 connectors plus one for each end electrode are required to address all 160 electrodes.

In this study, SU-8 2002 (Microchem, Newton, MA, USA), an epoxy based negative photoresist generally used to manufacture high aspect ratio microstructure, coated with a hydrophobic Cytop layer (Cytop CTL809M, Asahi Glass Co., Tokyo, Japan), was used as the functionalised dielectric. However, inherent process defects in the manufacture of SU-8 can result in microscopic pin-holes through the structure. These can cause direct contact between the chrome electrode and the droplet liquid, resulting in the first failure mechanism: electrochemical etching of the metal. The second failure mechanism, whilst uncommon, manifests itself by an electrical discharge between buried electrodes, caused by the electrical breakdown of SU-8. The use of ionic solutions in the actuated droplet (such as buffers) significantly increases the breakdown frequency of SU-8. This indicates possible ionic impregnation of the SU-8 layer resulting in the degradation of its dielectric properties. Both phenomena significantly reduce the base electrode lifetime and hence the reliability of the system.

Current work on a second generation device is aiming to improve the overall system reliability by using Parylene-C in addition to improving the engineering tolerance of the EWOD system. The result of this would be reduced droplet sticking and increased time between failures.

3. Test methodology

3.1. Characterisation of the ESP performance

For the testing of the ESP V1, a near mono-disperse aerosol of sodium fluorescein was produced using a modified vibrating orifice aerosol generator (VOAG) (TSI Inc., USA), where it was diluted with high efficiency particulate air (HEPA) filtered laboratory air, homogeneously mixed and aged using an aerosol containment and transfer system (ACATS). A proportion of the air was sampled by a tube which split the flow to a reference filter and the ESP. Iso-kinetic sampling allowed monitoring of the aerosol size distribution and concentration using an Aerodynamic Particle Sizer® (APS) 3321 (TSI Inc., USA). Both the ESP and the reference filter sampler operated at a flow rate of 5 L min^{-1}, controlled by mass flow controllers (Low DeltaP, Bronkhorst UK Ltd., UK). The aerosol sampled onto the reference filter and the collection electrode was washed off separately using a mixture of water and ethanol (1:1 v/v) which was subsequently analysed using a fluorimeter (LS-55 Fluorescence Spectrometer, PerkinElmer Inc., USA). The ESP collection efficiency was calculated by comparing the total mass of fluorescein in these two samples. The efficiency was tested with particles of mass median aerodynamic diameters (MMAD) from approximately 1.5 μm to 7.5 μm.

The collection efficiency of the ESP V2 was tested with and without porous foam in the inlet and was measured using sodium fluorescein aerosol generated using a flow focussing aerosol generator (FFAG) (Ganan-Calvo & Barrero, 1999) in conjunction with the ACATS. The ESP V2 was only tested with MMADs between 5 μm and 6 μm as the theory (Kenny et al., 2001; Vincent et al., 1993) suggests that there should be minimal effect on the efficiency for particles smaller than these.

The ESP V3 was tested using the same method as V2 and also with BG spore aerosol. The BG aerosol was generated using the FFAG. The quantity of BG removed from the ESP collection surface was then measured using real time polymerase chain

reaction (PCR) (using a previously characterised BG assay, Varughese, Wymer, & Haugland, 2007) and compared to reference filter data to give a collection efficiency. The BG particle MMAD was approximately 1.0 μm. BG recovery from the collection electrode was by means of a 1 mL rinse with de-ionised water or 90 s of shaking in 5 mL de-ionised water in a BD Falcon Centrifuge tube on a see-saw rocker.

3.2. EWOD surface cleaning efficiency

In order to test EWOD surface cleaning efficiency, ovalbumin (OA) and BG were deposited by sedimentation and by impaction respectively onto a hydrophobic collection surface. The BG used was tagged using fluorescein isothiocyanate (FITC) and the OA was tagged by mixing it with sodium fluorescein. The efficiency with which an EWOD actuated droplet removes deposited particulate from the hydrophobic collection surface was calculated by counting fluorescently tagged BG or OA particles on the surface before and after actuating a droplet.

3.3. Assessing the effect of droplet particle concentrations on actuation performance

It has been shown (Au, Kumar, & Wheeler, 2011; Luk, Mo, & Wheeler, 2008; Perry, Thomy, Das, Coffinierb, & Boukherroub, 2012) that when the concentration of material carried within a droplet becomes too high, the droplet can stick due to migration of the material to the surface, altering the local hydrophobicity. Although the effect that was reported was for smaller particles (proteins) than those considered here, a similar effect was observed in this work with BG spores. The droplet concentration threshold can be seen as analogous to a surface deposit concentration threshold, assuming that the droplet and surface concentration are in equilibrium.

The droplet concentration threshold should be compared to the limit of detection of the analysis method of interest, to ensure that a sufficiently high concentration can be achieved to trigger a detection alarm. This threshold is a possible weakness of the EWOD technique for aerosol collection applications.

The droplet concentration threshold was measured as follows. A defined concentration suspension or solution was produced. A droplet was taken from this stock material and an attempt to actuate it was made. Actuation performance was defined as the percentage of electrodes that the droplet could be actuated across. For this test, the actuation was 100% successful if the droplet could be actuated across the 16 electrodes of an EWOD test-bed. The maximum droplet concentration at which 100% actuation was achieved gives the concentration threshold. A droplet can therefore only be actuated across a surface up until the point at which it has collected sufficient material to reach this concentration threshold.

3.4. The electrostatic precipitator, EWOD system performance testing

The ESP-EWOD system efficiency was tested with BG spores and *Pseudomonas* phage 6 (Phi6). The ESP used in this test was V3 with an ion capture electrode; as discussed in Section 4.4. Both BG and Phi6 were aerosolised using the FFAG into the ACATS for 10 min. The collection surface from the ESP was then placed in the EWOD system and a droplet was actuated across the surface. The concentration of BG or Phi6 in the EWOD droplet was then measured using PCR. Phi6 samples were analysed by real time PCR using a newly designed Phi6 assay targeting the P2 polymerase gene, BG samples were analysed as described previously.

The Phi6 particle MMAD range measured in the ACATS was 1.08 μm *to* 1.13 μm and the BG range was 0.86 μm *to* 1.10 μm.

4. Results and discussion

4.1. Characterisation of the ESP performance

The collection efficiency for the ESP V1 with sodium fluorescein aerosol is shown in Fig. 4. Also shown is the predicted efficiency from the model described previously. The experimental data follows the theoretical curve down to approximately 2 μm where the spread of data suggests that the efficiency may drop faster than the theory predicts. The correlation between the experimental data and the theory supports the setting of $\eta_{c,max}$ to 0.85. The collection efficiency ranged from approximately 50% at 1.5 μm to greater than 80% above 4 μm.

Figure 5a shows the efficiency for the ESP V2 with sodium fluorescein aerosol, with two different 10 mm thick foam inlets (45 pores per inch (ppi) or 10 ppi) and for V2 without a foam inlet. Also included is the predicted efficiency curve. The limited data suggests that the 45 ppi foam reduced the efficiency whereas the 10 ppi foam had little effect.

The collection efficiency for ESP V3 with sodium fluorescein aerosol is shown in Fig. 5b. Two sets of data are shown: points for the ESP with no foam in the inlet and for a 10 mm thick 10 ppi foam. The three collection efficiency graphs indicate that the design modifications made between V1 and V3 did not have a detrimental effect on the collection efficiency.

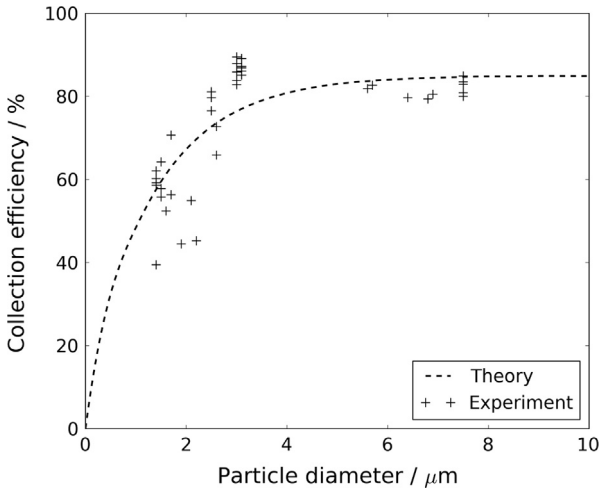

Fig. 4. Collection efficiency for the ESP V1 with sodium fluorescein aerosol, with each cross indicating a separate experimental result. Also included is the predicted efficiency (dashed line) calculated using (2).

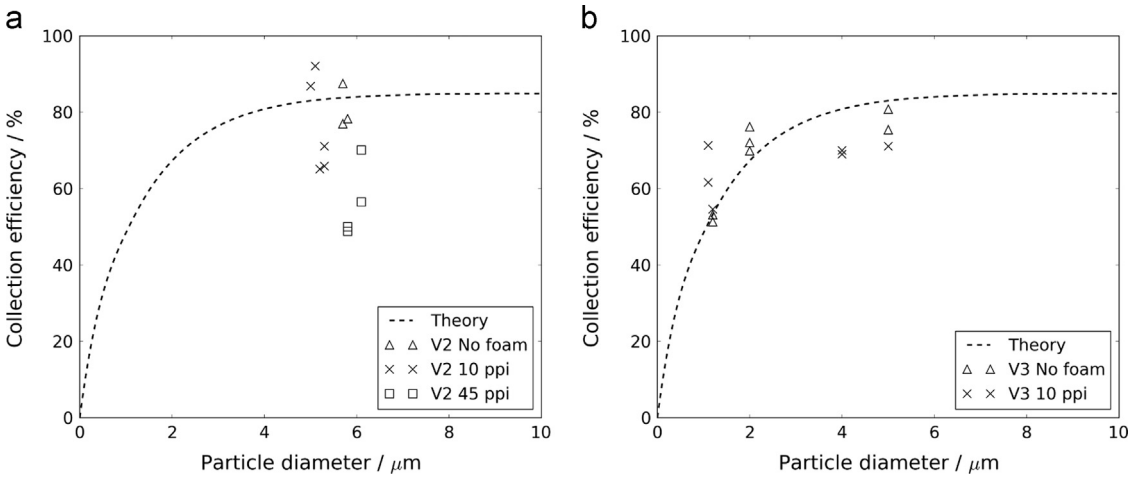

Fig. 5. The collection efficiency results for the ESP V2 and V3 with sodium fluorescein aerosol. (a) shows the effect of the foam inlet on the collection efficiency of ESP V2. The dashed curve is the theoretical efficiency curve. (b) is the collection efficiency of the ESP V3, again showing the theoretical efficiency curve.

The ESP V3 was characterised using BG spore aerosol. The indicative mean collection efficiency was 4.3% with a maximum of 10.2%. These values are lower than expected based on the theory and data for sodium fluorescein and are possibly due to different surface recovery rates for different types of aerosol and the surface damage discussed in Section 4.4.

4.2. EWOD surface cleaning efficiency

For BG particles, deposited by impaction, the cleaning efficiency varied from 80% to 98% (with an average of 93% based on measurements on three test surfaces) depending on the size of the deposited particles. The data showed that larger particles (i.e. those made up of more BG spores) were cleaned with a lower efficiency than smaller particles. These figures are higher that those reported by Jonsson-Niedziolka et al. (2011) which were 46% $\pm$ 16%.

For OA particles, the efficiency was harder to quantify. It was not clear whether OA that was previously clumped into a particle was being: fully removed, partially smeared across the surface and was no longer visible or the fluorescent tag was being washed off. Estimates for OA cleaning efficiency were greater than 80%.

4.3. The effect of droplet particle concentrations on actuation performance

The results from tests conducted using the method described in Section 3.3 are as follows. A 1.9 μL water droplet could be actuated with 100% success on a hydrophobic surface with OA concentrations up to 5 $\mu g\,mL^{-1}$ and with BG

concentrations up to 10^8 CFU mL^{-1}. If the surfactant Pluronic F127 (0.08% (w/w)) was added to the droplet then the OA threshold could be increased considerably to 1000 μg mL^{-1}. This increase was comparable to that reported by Luk et al. (2008) when Pluronic was added to protein carrying droplets. For BG, the presence of Pluronic reduced the actuation reliability. It is believed that lowering the surface tension decreased the ability of the droplet to collect and transport the solid object (i.e. the spores) from the surface resulting in actuation impairment.

4.4. The effect of corona ions on the hydrophobicity of the collection surfaces

During testing of the ESP V3 and the ESP-EWOD system the region of the hydrophobic collection surface directly opposite the corona pins was becoming hydrophilic after only five minutes of exposure to corona ions. This was discovered when water droplets that were placed in this region fully wetted the surface. The effect of plasmas or corona discharges directly rendering hydrophobic surfaces hydrophilic is well known within certain industries (Hillborg & Gedde, 1998; Widmer, Heuberger, Voros, & Spencer, 2001).

A basic modification was made to the ESP V3 to allow for ESP-EWOD system efficiency testing to be conducted and to assess how easily the issue could be avoided. An additional raised ion capture electrode was added to the upstream section of the collection surface and the ESP V3 flow rate was increased from 5 L min^{-1} to 20 L min^{-1} to reduce aerosol loss to the protecting electrode. The ion-capture electrode was held at the same voltage as the collection electrode.

The ion capture electrode will have the undesirable effect of removing some charged aerosol particles before they reach the hydrophobic surface therefore reducing the system efficiency. The increase in flow rate will also have an effect on the efficiency.

With this modification, the surface was no longer becoming hydrophilic during a 10 min test period. This confirmed that the surface damage was due to ions and also that a permanent solution to the problem should be achievable. More complete separation of charging and collection regions in a next generation ESP would stop the surface damage. It is expected that the ESP could be designed in a way that would cause minimal detrimental effect on the aerosol collection efficiency.

The increase in flow rate was taken into account for the calculation of the system efficiency and concentration rate shown in Table 2.

4.5. The electrostatic precipitator, EWOD system performance

The ESP-EWOD system efficiency data and concentration rate (using ESP V3 with the ion capture electrode) is shown in Table 2. The system efficiency measured with BG was based on five tests and the Phi6 based on two tests.

The mean concentration rates given in Table 2 range from approximately 15 to 35 times less than the theoretical maximum concentration rate given in Table 1 for the ESP-EWOD system operating at 20 L min^{-1}. If the ESP design could be modified so that the temporary ion capture electrode is no longer required, then it is believed that it should be possible to achieve a system efficiency for BG, of approximately 32%. This estimate is based on the following two assumptions: that BG is collected as efficiently as sodium fluorescein i.e. approximately 35% at 1 μm (see Fig. 4); and the surface cleaning efficiency is at least as high as the average measured earlier, i.e. 93% (see Section 4.2). The resulting system efficiency, η_s, is 35% $\times$ 93%. It should be noted that this efficiency would only be achievable while the particle concentration in the actuated droplet is below the threshold concentration described in Section 4.3.

Even with the negative effect of the ion capture electrode, the concentration rate of the prototype ESP-EWOD system is already an order of magnitude higher than (the theoretical maximum of) the best COTS personal sampler presented in Table 1. This highlights the merit in the ESP-EWOD concept for personal sampling of aerosol and points towards the advantages that would be achievable in a more fully functioning system.

5. Conclusions

A prototype lightweight personal electrostatic precipitator has been built and has performed well under test. The collection efficiency ranged from 50% at 1.5 μm to greater than 80% above 4 μm for sodium fluorescein aerosol and 4.3% for BG spores (0.98 μm). A compact, semi-automated EWOD module to receive the collection surfaces from the ESP and to actuate microlitre size droplets across the collection surface has been built. The actuated droplet efficiently collects previously deposited aerosol resulting in a high concentration sample. The prototype ESP-EWOD system, when tested with BG spores,

Table 2
The ESP-EWOD system efficiency, η_s, (using ESP V3 with the ion capture electrode and a flow rate of 20 L min^{-1}) and mean concentration rate, R_c, for BG and Phi6. All data is based on a single pass of the EWOD actuated droplet.

Simulant	Minimum η_s/%	Maximum η_s/%	Mean η_s/%	Mean R_c/min^{-1}
BG	1.34	5.42	2.71	1.9×10^5
Phi6	1.55	11.08	6.32	4.4×10^5

had an average concentration rate of 1.9×10^5 min^{-1} and an average system efficiency of 2.7%. For Phi6, the average concentration rate was 4.4×10^5 min^{-1} and the average system efficiency was 6.3%.

A weakness in the ESP-EWOD integration caused by corona ions damaging the hydrophobic surface has meant that ESP-EWOD system tests showed a lower efficiency and concentration rate than expected. Current work on a second generation device is addressing this issue. However, even with this low efficiency the system shows significant advantages over COTS personal samplers. Its measured concentration rate is approximately an order of magnitude higher than the theoretical maximum of the next best personal sampler system, increasing the likelihood of providing a sample which could trigger a detector.

When the concentration of particles within a droplet becomes too high, the droplet will stick due to migration of the material to the surface, altering the local hydrophobicity. The significance of this effect has been explored but it remains a possible weakness of the current EWOD technique for aerosol collection applications. The droplet concentration thresholds, up to 5 μg mL^{-1} for OA and up to 10^8 CFU mL^{-1} for BG, should be compared to the limit of detection of the analysis method of interest to ensure that a sufficiently high concentration can be achieved.

Finally, an ESP-EWOD based personal sampler system has the additional advantage that it would lend itself well to future automation and integration with a lab-on-a-chip type identification system.

Acknowledgments

The research was supported by the UK Ministry of Defence.

References

Arelco (2014). Capteur individuel de pollutants microbiologiques. ⟨http://www.tecora.com/en/health-and-safety/1205-cip10-m.html⟩ Accessed 27.06.14.
Au, S., Kumar, P., & Wheeler, A. (2011). A new angle on pluronic additives: Advancing droplets and understanding in digital microfluidics. *Langmuir* 27.
Choi, K., Ng, A., Fobel, R., Chang-Yen, D., Yarnell, L., Pearson, E., et al. (2013). Automated digital microfluidic platform for magnetic-particle-based immunoassays with optimization by design of experiments. *Analytical Chemistry*, *85*, 9638–9646.
Christensen, L., Brehm, K., Skov, J., Harlow, K., Christensen, J., & Haas, B. (2009). Detection of foot-and-mouth disease virus in the breath of infected cattle using a hand-held device to collect aerosols. *The Veterinary Journal*, *179*.
Clark, J., Foat, T., Walker, M., & Preston, S. (2008). Electrostatic precipitator. US Patent 7,361,212.
Cross, J. (1987). *Electrostatics, principles, problems and applications*. Bristol, UK: Institute of Physics Publishing.
Delattre, C., Allier, C., Fouillet, Y., Jary, D., Bottausci, F., Bouvier, D., et al. (2012). Macro to microfluidics system for biological environmental monitoring. *Biosensors and Bioelectronics*, *36*, 230–235.
Fair, R., Khlystov, A., Srinivasan, V., Pamula, V., & Weaver, K. (2004). Integrated chemical/biochemical sample collection, pre-concentration, and analysis on a digital microfluidic lab-on-a-chip platform. In *Proceedings of the SPIE 5591, Lab-on-a-Chip: platforms, devices, and applications* (Vol. 113).
Flir (2014). Biobadge 100 portable personal aerosol sampler—Product overview. ⟨http://gs.flir.com/uploads/file/products/brochures/biobadge.pdf⟩ Accessed 27.06.14.
Franz, D., Jahrling, P., & Friedlander, A. (1997). Clinical recognition and management of patients exposed to biological warfare agents. *Journal of the American Medical Association*, *278*(5).
Ganan-Calvo, A., & Barrero, A. (1999). A novel pneumatic technique to generate steady capillary microjets. *Journal of Aerosol Science*, *30*, 117–125.
Gorner, P., Fabries, J.-F., Duquenne, P., Witschger, O., & Wrobel, R. (2006). Bioaerosol sampling by a personal rotating cup sampler CIP 10-M. *Journal of Environmental Monitoring*, *8*, 43–48.
Gorner, P., Simon, X., Wrobel, R., Kauffer, E., & Witschger, O. (2010). Laboratory study of selected personal inhalable aerosol samplers. *Annals of Occupational Hygiene*, *54*(2), 165–187.
Han, T., An, H., & Mainelis, G. (2010). Performance of an electrostatic precipitator with superhydrophobic surface when collecting airborne bacteria. *Aerosol Science and Technology*, *4*, 339–348.
Han, T., & Mainelis, G. (2008). Design and development of an electrostatic sampler for bioaerosols with high concentration rate. *Aerosol Science and Technology*, *39*, 1066–1078.
Hillborg, H., & Gedde, U. (1998). Hydrophobicity recovery of polydiethylsiloxane after exposure to corona discharges. *Polymer*, *39*.
Jönsson-Niedziółka, M., Lapierre, F., Coffinier, Y., Parry, S., Zoueshtiagh, F., Foat, T., et al. (2011). EWOD cleaning of bioparticles on hydrophobic and superhydrophobic surfaces. *Lab on a Chip*, *11*.
Kenny, L., Aitken, R., Beaumont, G., & Gorner, P. (2001). Investigation and application of a model for porous foam aerosol penetration. *Journal of Aerosol Science*, *232*.
Kim, H., Bartsch, M., Renzi, R., He, J., de Vreugde, J. V., Claudnic, M., et al. (2011). Automated digital microfluidic sample preparation for next-generation dna sequencing. *Journal of Laboratory Automation*, *16*(6), 405–414.
Kirby, A., & Wheeler, A. (2013). Digital microfluidics: An emerging sample preparation platform for mass spectrometry. *Analytical Chemistry*, *85*, 6178–6184.
Ko, S., Lee, H., & Kang, K. (2008). Hydrodynamic flows in electrowetting. *Langmuir*, *24*.
Luk, V. N., Mo, G., & Wheeler, A. (2008). Pluronic additives: A solution to sticky problems in digital microfluidics. *Langmuir*, *24*.
Mainelis, G., Adhikari, A., Willeke, K., Lee, S.-A., Reponen, T., & Grinshpun, S. (2002). Collection of airborne microorganisms by a new electrostatic precipitator. *Aerosol Science*, *33*, 1417–1432.
Miller, A., Frey, G., King, G., & Sunderman, C. (2010). A handheld electrostatic precipitator for sampling airborne particles and nanoparticles. *Aerosol Science and Technology*, *44*, 417–427.
Nelsen, W., Peng, I., Lee, G.-A., Loo, J., Garrell, R., & Kim, C.-J. (2010). Incubated protein reduction and digestion on an electrowetting-on-dielectric digital microfluidic chip for maldi-ms. *Analytical Chemistry*, *82*, 9932–9937.
Ningsi, M. (2014). *A digital microfluidic platform for human plasma protein depletion* (Master's thesis). Queens University, Canada.
Oh, J., Ko, S., & Kang, K. (2008). Shape oscillation of a drop in ac electrowetting. *Langmuir*, *24*, 8379–8386.

Perry, G., Thomy, V., Das, M., Coffinier, Y., & Boukherroub, R. (2012). Inhibiting protein biofouling using graphene oxide in droplet-based microfluidic microsystems. *Lab on a Chip*, *9*.
Qi, C., Chen, D., & Greenberg, P. (2008). Fundamental study of a miniaturized disk-type electrostatic aerosol precipitator for a personal nanoparticle sizer. *Aerosol Science and Technology*, *42*, 505–512.
Quinton, E., Achard, J.-L., & Roux, J.-M. (2013). Ionic wind generator derived from a liquid filled capillary pin. Application to particle capture. *Journal of Electrostatics*, *71*.
Rose, H., & Wood, A. (1956). *An introduction to electrostatic precipitation in theory and practice*. London, UK: Constable and Company Ltd.
Roux, J.-M., Kaspari, O., Heinrich, R., Hanschmann, N., & Grunow, R. (2013). Investigation of a new electrostatic sampler for concentrating biological and non-biological aerosol particles. *Aerosol Science and Technology*, *47*, 463–471.
Ryan, E., Wright, C., & Gloster, J. (2009). Measurement of airborne foot-and-mouth disease virus: Preliminary evaluation of two portable air sampling devices. *The Veterinary Journal*, *179*(3).
Sarda-Esteve, R., Roux, J.-M., Sciare, J., Delapierre, G., & Nadal, M. -H. (2012). Collection efficiency of a newportable electrostatic precipitator (BIODOSI) designed for the collection of airborne pathogens. In *AAAR conference*, Minneapolis, USA.
Sillanpää, M., Geller, M., Phuleria, H., & Sioutas, C. (2008). High collection efficiency electrostatic precipitator for in vitro cell exposure to concentrated ambient particulate matter (pm). *Aerosol Science*, *39*, 335–347.
SKC, (2014a). Button aerosol sampler. ⟨http://www.skcinc.com/prod/225-360.asp⟩ Accessed 27.06.14.
SKC, (2014b). Personal environmental monitor. ⟨http://www.skcinc.com/prod/761-200.asp⟩ Accessed 27.06.14.
SKC, N.D. IOM personal sampler and IOM sampler with MultiDust—Operating instructions. Technical report. Form 37372 Rev 0607, SKC.
Sleeth, D., & Vincent, J. (2012). Performance study of personal inhalable aerosol samplers at ultra-low wind speeds. *Annals of Occupational Hygiene*, *56*(2), 207–220.
Tan, M., Shen, F., Yao, M., & Zhu, T. (2010). Development of an automated electrostatic sampler (aes) for bioaerosol detection. *Aerosol Science and Technology*, *4*, 339–348.
Varughese, E., Wymer, L., & Haugland, R. (2007). An integrated culture and real time pcr method to assess viability of disinfectant treated bacillus spores using robotics and the mpn quantification method. *Journal of Microbiological Methods*, *71*, 66–70.
Vincent, J. (2007). *Aerosol sampling*. Chichester, UK: Wiley.
Vincent, J., Aitken, R., & Mark, D. (1993). Porous plastic foam filtration media: Penetration characteristics and applications in particle size-selective sampling. *Journal of Aerosol Science*, *24*(7), 55.
Volckens, J., Boundy, M., & Leith, D. (2000). Mist concentration measurements. ii: Laboratory and field evaluations. *Applied Occupational and Environmental Hygiene*, *15*(4), 370–379.
Volckens, J., Leith, D., Boundy, M., & Hands, D. (1999). Oil mist concentration: A comparison of sampling methods. *American Industrial Hygiene Association Journal*, *60*, 684–689.
Widmer, M., Heuberger, M., Voros, J., & Spencer, N. (2001). Influence of polymer surface chemistry on frictional properties under protein-lubrication conditions: Implications for hip-implant design. *Tribology Letters*, *10*.
Zhao, Y., & Cho, S. (2006). Microparticle sampling by electrowetting-actuated droplet sweeping. *Lab on a Chip*, *6*, 137–144.